Quantum-Classical Dual Kernel SVMs for Power Quality Classification

Dhana Phassadawongse[0009−0000−8412−0963]
and Stephen John Turner[0000−0002−7421−9801]

Vidyasirimedhi Institute of Science and Technology (VISTEC), Rayong, 21210, Thailand
{dhana.p_s24,steve.t}@vistec.ac.th

Abstract. Quantum Machine Learning (QML) has emerged as a promising field at the intersection of quantum computing and Machine Learning (ML), offering new possibilities for enhanced data processing and classification tasks. In particular, quantum kernel methods have demonstrated potential advantages over their classical counterparts in high-dimensional feature mapping. In the transition toward more sustainable energy, Power Quality Disturbance (PQD) classification is crucial for ensuring grid stability amid growing renewable energy integration. Rapid and accurate detection of disturbances enables timely corrective actions to maintain reliable power supply. Support Vector Machines (SVMs), a class of supervised ML models based on kernel methods, have been widely used for PQD classification due to their strong generalization capabilities. In this paper, we integrate a quantum approach into the SVM framework and propose a novel quantum-classical dual kernel SVM that outperforms both purely classical and purely quantum kernel SVMs on an S-transform PQD dataset. By incorporating a weighting strategy between classical and quantum kernels, we develop a robust and highly accurate PQD classification model, achieving an average accuracy of 98.46% across all noise levels. To the best of our knowledge, this is the first application of a quantum-classical dual kernel SVM in power system applications, thereby demonstrating QML's potential to enhance real-world classification.

Keywords: Quantum machine learning · Support vector machine· Power quality disturbance · Classification.

1 Introduction

Quantum computing exploits core quantum phenomena—superposition, entanglement, and interference—to enable computations that can exceed classical capabilities in certain domains. By leveraging superposition, a qubit can represent multiple states simultaneously, providing quantum parallelism and thereby facilitating more efficient pattern recognition. Entanglement further enriches feature encoding by creating strong correlations among qubits, enhancing optimization

and machine learning in complex models. Recent advancements have demonstrated that quantum machine learning (QML) can harness these quantum effects to improve tasks such as classification, clustering, and kernel-based learning beyond that possible with purely classical methods [5]. To achieve this, Havlíček et al. [11] and Schuld [23] independently observed how data features could be mapped into a potentially infinite-dimensional space by introducing a quantum feature map that enables feature separability utilizing a kernel method, leading to improved classification performance in supervised ML techniques, especially in support vector machines (SVMs).

One crucial application is the classification of power quality disturbances (PQDs). PQDs arise when key electrical signal waveform parameters—both magnitude and frequency—deviate from nominal operating conditions. These deviations, or distortions, can significantly degrade the reliability and stability of the power grid, potentially leading to equipment damage [2], blackouts, and costly downtime for industrial and commercial operations [4]. Addressing PQDs is especially critical in modern grids that integrate variable renewable energy (VRE) sources, such as solar and wind. While these sources reduce greenhouse gas emissions, their dependence on intermittent natural energy inputs exacerbates waveform distortions, including harmonics, flicker, and other fluctuations in the grid [10, 29]. Distributed generation, including rooftop solar photovoltaics (PV) and local wind turbines, further amplifies these disturbances, especially at the district utility level [1, 9, 27]. Accurately detecting and classifying diverse PQD types requires robust analytical methods, as the main challenge lies in distinguishing multiple overlapping disturbance signals. Failure to address these disturbance types accurately can lead to significant economic losses, making PQD classification a crucial concern for safeguarding grid reliability and efficiency.

In this paper, we introduce a quantum-classical dual kernel SVM, a novel approach that seamlessly integrates quantum computing into the traditional SVM framework to enhance PQD classification. By leveraging a dynamic weighting strategy between classical and quantum kernels, our model effectively captures complex and overlapping features in PQD data, leading to superior classification performance. Our method outperforms both purely classical and purely quantum kernel SVMs, achieving a remarkable 98.46% average accuracy across all noise levels. Our results demonstrate that this quantum-classical dual kernel approach successfully balances the strengths of both paradigms across various hyperparameters and noise levels in PQD datasets, paving the way for more robust and accurate PQD classification in modern power systems.

This paper is organized as follows. Section 2 discusses related work in PQD classification, using either classical or quantum ML techniques. In Section 3, the SVM formulation is briefly discussed for classification purposes, together with classical and quantum kernel methods. Section 4 presents our quantum-classical dual kernel method in PQD classification. In Section 5, experimental results are presented and analyzed followed by conclusions in Section 6.

2 Related Work

ML techniques have significantly enhanced the accuracy and adaptability of PQD classification. Review articles [3, 7, 19, 22] offer critical and comprehensive discussions of a wide range of power quality (PQ) feature extraction methods and PQD classifiers. Notably, SVMs stand out for their effectiveness in handling large feature sets and delivering robust and stable classification results. In PQD classification, Cerqueira et al. [8] used SVMs to demonstrate an improved performance in classifying standard types of PQD compared to traditional methods such as optimal time-frequency representation (OTFR).

In PQD feature analysis and extraction, Igual et al. [14] used the Stockwell transform (S-transform) [25] on synthetic PQD datasets yielding both time and frequency resolutions of PQDs as they provide localized information about the disturbances which are time- and frequency-varying in nature. In general, PQD types are addressed in accordance with IEEE Recommended Practice for Monitoring Electric Power Quality [12].

For classical kernel SVMs, Lin et al. [18] presented a multiclass one-versus-one (OvO) SVM application in PQD classification and demonstrated that the results were better than those of an artificial neural network (ANN) on the IEEE 14-bus power system with seven PQD types. Similarly, Borrás et al [6] applied an OvO-based SVM to classify disturbance ratios for optimal multi-event classification in power distribution networks, achieving an average accuracy of 94.2%. Furthermore, Tang et al. [26] conducted extensive experiments to verify a composite (linearly combined) kernel function, with time, frequency, and raw PQD signals as features assigned to each of the three kernels, on different noise levels across 24 PQD features. When using traditional S-transform data with the kernel SVM method alone, they achieved an average accuracy of 94.71%.

While classical ML methods have been widely used for PQD classification, recent advancements in QML techniques [17] have introduced new possibilities for improving classification accuracy, In particular, the quantum kernel method exhibits matrix computations similar to those in classical kernel-based SVMs, giving rise to quantum SVM for regression and classification tasks.

Wang et al. [28] introduced what they claimed to be the first application of quantum SVM (QSVM) as a QML approach, based on one-versus-the-rest (OvR) binary classification approach, to classify seven types of PQD under different noise conditions, achieving accuracy in the range of 87% to 95%. The main focus of their paper is the training time, achieving a superior time complexity of $O(n^2 log(n))$ compared to classical SVM.

3 Support Vector Machine

SVMs are a type of supervised learning algorithm used for classification tasks. In this setting, each training sample is provided as a pair $\{(\mathbf{x}_i, y_i)\}_{i=1}^{N}$, where $\mathbf{x}_i \in \mathbb{R}^d$ is a d-dimensional feature vector representing the input data and $y_i \in \{-1, +1\}$ is its corresponding binary label indicating class membership.

3.1 Soft-Margin SVM Formulation

For datasets that are not perfectly separable, the soft-margin SVM seeks to find a hyperplane that maximizes the margin while allowing some misclassifications. In this formulation, the model parameters include the weight vector $\mathbf{w}$, which is perpendicular to the hyperplane, and the bias b that shifts the hyperplane. Slack variables $\xi_i \geq 0$ are introduced to permit violations of the margin constraints, and $C > 0$ is a regularization parameter controlling the trade-off between margin maximization and the penalty for misclassifications.

The primal optimization problem is formulated as

$$\min_{\mathbf{w},\, b,\, \boldsymbol{\xi}} \ \frac{1}{2}\|\mathbf{w}\|^2 + C\sum_{i=1}^{N} \xi_i \quad \text{subject to} \quad y_i(\mathbf{w}^\top \mathbf{x}_i + b) \geq 1 - \xi_i, \quad \xi_i \geq 0, \tag{1}$$

which minimizes the norm of $\mathbf{w}$ (thus maximizing the margin) while penalizing the slack variables ξ_i scaled by C. By applying Lagrangian duality with multipliers α_i for each constraint, the dual form is obtained as

$$\begin{aligned} \max_{\boldsymbol{\alpha}} \quad & \textstyle\sum_{i=1}^{N} \alpha_i - \frac{1}{2}\sum_{i,j=1}^{N} \alpha_i\, \alpha_j\, y_i y_j\, K(\mathbf{x}_i, \mathbf{x}_j) \\ \text{subject to} \quad & \textstyle\sum_{i=1}^{N} \alpha_i y_i = 0, \\ & 0 \leq \alpha_i \leq C, \quad i = 1, \ldots, N. \end{aligned} \tag{2}$$

Here, α_i are the Lagrange multipliers corresponding to each training example, and the kernel function $K(\mathbf{x}_i, \mathbf{x}_j)$ replaces the inner product $\mathbf{x}_i^\top \mathbf{x}_j$ to enable the method to operate in a high-dimensional feature space, thereby constructing non-linear decision boundaries. The constraint $\sum_{i=1}^{N} \alpha_i y_i = 0$ ensures that the solution appropriately balances the contributions of both classes.

3.2 Kernel Methods in SVM

Although linear SVMs can be effective, many real-world datasets—such as those involving PQDs—exhibit non-linear relationships that cannot be adequately captured by a single linear decision boundary. To address this, SVMs leverage kernel functions to implicitly map data into higher-dimensional feature spaces where linear separation is more likely.

Kernel Trick Rather than explicitly computing the transformed coordinates of each data point, SVMs employ pairwise kernel evaluations. Given a mapping $\phi : \mathbb{R}^d \to \mathcal{H}$, from Mercer's theorem [20], the kernel function is defined as

$$K(\mathbf{x}_i, \mathbf{x}_j) \ = \ \big\langle \phi(\mathbf{x}_i),\, \phi(\mathbf{x}_j) \big\rangle. \tag{3}$$

This approach, known as the kernel trick, allows one to compute the inner products in $\mathcal{H}$ without explicitly forming the mapping $\phi(\mathbf{x})$ which is computationally expensive.

Common Kernel Functions Various kernel functions have been employed successfully in classification tasks:

Linear Kernel: This is the simplest kernel, often serving as a baseline or used when data is close to linearly separable. The kernel is defined as

$$K(\mathbf{x}_i, \mathbf{x}_j) = \mathbf{x}_i^\top \mathbf{x}_j. \tag{4}$$

Radial Basis Function (RBF) Kernel: This kernel can capture localized non-linear relationships and is frequently used when the data has complex boundaries. The kernel is defined as

$$K(\mathbf{x}_i, \mathbf{x}_j) = \exp\big(-\gamma \|\mathbf{x}_i - \mathbf{x}_j\|^2\big). \tag{5}$$

Polynomial Kernel: It encapsulates polynomial relationships of degree d, with c controlling the relative contribution of higher-order terms. The kernel is defined as

$$K(\mathbf{x}_i, \mathbf{x}_j) = \big(\mathbf{x}_i^\top \mathbf{x}_j + c\big)^d. \tag{6}$$

Regardless of the specific kernel, the SVM training process remains the same; only the dot products in the optimization problem are replaced by kernel evaluations, providing a powerful and flexible framework for capturing complex patterns in data.

3.3 Quantum Feature Maps and Kernel Computation

Quantum Feature Maps A mapping $\phi : \mathcal{X} \to \mathcal{H}$, where $\mathcal{X} \subseteq \mathbb{R}^d$ is a classical input space and $\mathcal{H}$ is a quantum Hilbert space, is called a quantum feature map. The map ϕ transforms classical data $\mathbf{x} \to |\phi(\mathbf{x})\rangle$ for all $\mathbf{x} \in \mathcal{X}$ where $|\phi(\mathbf{x})\rangle$ are features in quantum space. In practice, this is realized by a parameterized quantum circuit $U(\mathbf{x})$ acting on an n-qubit reference state $|0\rangle^{\otimes n}$:

$$|\phi(\mathbf{x})\rangle \;=\; U(\mathbf{x})\; |0\rangle^{\otimes n}\,. \tag{7}$$

Since an n-qubit system spans a Hilbert space of dimension 2^n, even moderate n can yield extremely high-dimensional encodings compared to classical feature maps.

Typical encodings allow each component of $\mathbf{x} = (x_1, \ldots, x_d)$ to parameterize single-qubit or multi-qubit gates, such as rotations $R_z(x_j)$, or more complex entangling operations. The aim is to exploit quantum phenomena (e.g., superposition and entanglement) so that the resulting feature map captures non-trivial relationships in data that may be difficult to represent classically.

Feature Map Encoding One commonly used quantum feature map is the *ZZFeatureMap*, which repeats a parameterized circuit pattern over several layers or repetitions. Formally, we can write:

$$U_{\mathrm{ZZ}}(\mathbf{x}) \;=\; \prod_{k=1}^{r} \Big[\, U_{\mathrm{ent}}(\theta_k)\, U_{\mathrm{rot}}(\mathbf{x}) \Big], \tag{8}$$

where r is the number of *repetitions*, $U_{\mathrm{rot}}(\mathbf{x})$ typically encodes the input features $\mathbf{x}$ as single-qubit rotations, and $U_{\mathrm{ent}}(\theta_k)$ applies an *entanglement pattern* (e.g., linear, circular, or full) among the qubits. By adjusting both r and the entanglement pattern, we control how strongly the feature map exploits quantum correlations:

- *Repetition* Increasing r repeats the encoding and entangling layers multiple times, potentially creating richer quantum states that capture higher-order interactions.
- *Entanglement Pattern* Defines which qubits become entangled. Common options include:
  - *Linear* Connects qubits in a chain, e.g., 1–2, 2–3, etc.
  - *Circular* Connects qubits in a ring, e.g., 1–2, 2–3, ..., $(n-1)$–n, and n–1.
  - *Full* Applies entangling gates between *all* pairs of qubits.

These hyperparameters (r and the entanglement pattern) can be tuned to balance expressivity against hardware noise and computational overhead. In practice, choosing an overly complex entangling scheme or too many repetitions may lead to vanishing gradients.

Quantum Kernel Computation Once two data points $\mathbf{x}$ and $\mathbf{x}'$ are mapped to the quantum states $|\phi(\mathbf{x})\rangle$ and $|\phi(\mathbf{x}')\rangle$, we define the *quantum kernel* as the squared magnitude of their overlap:

$$K_q(\mathbf{x}, \mathbf{x}') \;=\; \big|\langle \phi(\mathbf{x}) \mid \phi(\mathbf{x}')\rangle\big|^2. \tag{9}$$

In our proposed quantum-classical dual kernel SVM framework, we linearly combine the quantum kernel with an hyperparameter-tuned classical kernel, thereby harnessing the complementary strengths of both paradigms. In the following section, we explain PQD classification with the dual kernel SVM methodology.

4 Quantum-Classical Dual Kernel Methodology

4.1 Power Quality Disturbance Datasets

Datasets The S-transform PQD datasets are directly acquired from the IEEE Dataport repository [13] based on the work of Igual et al. [14] discussed in Section 2. The datasets comprise nine PQD types: normal, sag, swell, interruption,

oscillatory transient, harmonics, voltage fluctuation, sag with harmonics, and swell with harmonics. To reflect real-world scenarios, different signal-to-noise ratios (SNR) are incorporated into each dataset—namely, noiseless, 50 dB, 40 dB, 30 dB, and 20 dB—arranged in ascending order of noise level.

Features Each dataset includes eight features derived from the S-transform of synthetic PQD signals, yielding a time-frequency matrix [25]. The important features of the S-transform matrix are expressed in terms of Time-maximum-Amplitude (TmA) and Frequency-maximum-Amplitude (FmA) plots as described in Table 1.

Table 1. Description of S-transform-derived time-frequency features

Feature	Description
1	Average absolute value of the S-transform matrix row
2	Standard deviation of TmA-plot
3	Maximum value of TmA-plot
4	Minimum value of TmA-plot
5	Number of peaks in the TmA-plot
6	Standard deviation of FmA-plot between the 3^{rd} and 7^{th} harmonics
7	Standard deviation of FmA-plot above the 3^{rd} harmonic
8	Number of points near zero in one cycle minus the typical number of points found in an undistorted signal

4.2 Classification Workflow and Techniques

Data Preparation The raw data, stored in comma-separated value (CSV) format, are organized into directories based on their noise level (noiseless, 50 dB, 40 dB, 30 dB, and 20 dB). Each CSV file contains the eight S-transform-derived features for a specific PQD type. The file-naming convention uses an initial numeric label indicating the PQD type, which is extracted and used as the ground truth label during processing. CSV files are read using the defined feature columns and sorted by the numeric label at the start of each filename. This ensures that the label associated with each dataset is correctly assigned.

Data Preprocessing After loading, individual files are concatenated into a single `DataFrame` per noise level. The raw feature data are then preprocessed through a pipeline implemented in `Scikit-learn` [21]. In this study, experiments are carried out using 75% of the data as training while the remaining 25% is used for kernel testing. The pre-processing steps shown in Figure 1 include: 1) `StandardScaler` normalizes the features to zero mean and unit variance, 2) Principal Component Analysis (PCA) reduces dimensionality while retaining 95% of the variance, and 3) `MinMaxScaler` rescales the PCA-transformed data into the $[0, 1]$ range, which can be advantageous for subsequent model training.

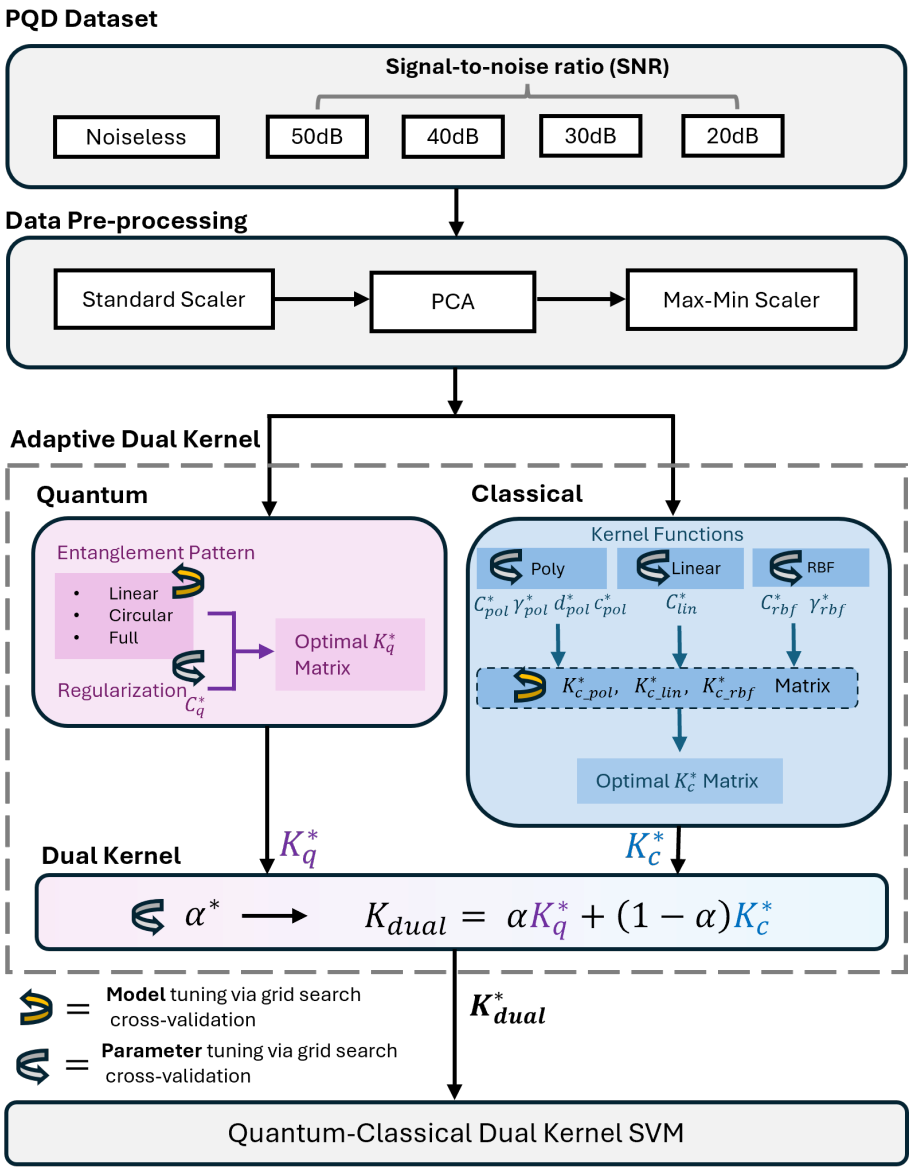

Fig. 1. Quantum-Classical Dual Kernel SVM Workflow with Adaptive Model and Parameter Tuning

4.3 Quantum-Classical Dual Kernel Training

Classical Kernel In the classical kernel setting, we explore three kernel functions from equations (4) to (6) by using multi-class one-versus-one (OvO) SVM function in `Scikit-learn` libraries to capture the decision boundary in a high-dimensional, implicitly mapped feature space. Their corresponding hyperparameters are tuned for the best result.

Quantum Kernel To harness potential quantum advantages, we adopt a quantum kernel method that computes a *kernel matrix* from feature-encoded quantum states. Specifically, we use `FidelityStatevectorKernel` to measure the overlap (fidelity) between any two quantum states as in equation (9). IBM Qiskit [16] provides a quantum kernel interface which is compatible with `Scikit-learn` and uses the same multi-class SVM approach. This enables accurate estimation of the quantum kernel which can be plugged into the kernel term in equation (2). In this way, we can explore the regularization parameter C of three different entanglement patterns of a quantum kernel.

Dual Kernel To leverage the strengths of both kernels, we propose a quantum-classical dual kernel approach which linearly combines the quantum kernel matrix K_q with a classical kernel matrix K_c:

$$K_{\text{dual}} \;=\; \alpha\, K_q \;+\; (1-\alpha)\, K_c, \tag{10}$$

where $\alpha \in [0,\, 1]$ is a weighting parameter balancing quantum against classical contributions by adaptively tuning α based on grid search cross-validation performance. The details of model and hyperparameter tuning are given in the next section.

5 Experimental Results and Analysis

5.1 Model and Parameter Tuning in Dual Kernel SVM Workflow

In Table 2, we present the models and their detailed hyperparameter tuning results in each kernel by showing their classification accuracy under severe 20 dB signal-to-noise ratio (SNR) PQD dataset. In the quantum kernel, with two repetitions, the Circular entanglement pattern achieves the highest accuracy at 92.90%. In the classical kernel, the polynomial (poly) kernel demonstrates the best standalone performance of 92.60% with its respective optimal hyperparameters. Finally, in the dual kernel, the best-performing combination for 20 dB SNR is the dual Circular—poly kernel with 93.49% mean accuracy.

5.2 Overall Performance of Adaptive Dual Kernel

Table 3 shows that the adaptive quantum-classical dual kernel achieves a higher accuracy across all noise levels than any single kernel alone. Ultimately, this adaptive approach maintains a robust overall average accuracy of 98.46% (std. dev. 2.80%) across different noise conditions.

Table 2. Models and Parameters Tuning in Dual Kernel Method Under 20 dB SNR

PQD data with 20 dB SNR								
Quantum			**Classical**					
Entanglement	C_q^*	Acc.(%)	Kernel	C_k^*	d^*	γ^*	c^*	Acc.(%)
Linear	10	91.12	linear	100	-	-	-	92.31
Circular	10	92.90	poly	100	4.0	1.0	0.0	92.60
Full	10	91.12	rbf	100	-	1.0	-	92.60
Dual kernel with varying α								
Quantum (Circular) — Classical (poly)				0.10	0.30	0.45	0.70	0.90
Accuracy (%)				92.90	93.20	93.49	93.20	92.90
		Best Dual Kernel Acc.			93.49%			

Table 3. Overall Performance of Adaptive Quantum-Classical Dual Kernel Across Noise Levels

Quantum		**Classical**		**Quantum-Classical Dual Kernel**	
K_q	Acc.(%)	K_c	Acc.(%)	K_{dual}	Mean ± Std. Dev.
Linear	97.69	linear	97.45	Adaptive Dual Kernel Acc.	98.46% ± 2.80%
Circular	97.99	poly	98.28		
Full	97.10	rbf	97.93		

5.3 Performance Under Different Noise Levels

In Table 4, we illustrate the adaptive performance of three quantum kernels with different entanglement patterns and three classical kernels for each level of noise in the PQD datasets, together with the optimal dual kernel weighting parameter α. Despite variations in noise levels, the dual approach consistently delivers high performance. The small standard deviations indicate that the accuracy is robust and stable across different experimental settings. Whereas other noise levels have a narrow range or an optimal value of α, the noiseless and 50 dB noise conditions exhibit a wide range of α.

6 Conclusions

In this paper, we analyze the performance of a quantum-classical dual kernel on S-transform synthetic PQD datasets, which comprise the nine most common disturbances at different noise levels. Results indicate that the dual kernel method performs better than either quantum or classical kernels in terms of accuracy using an adaptive tuning method. With an overall dual kernel accuracy averaging 98.46% over an optimal range of weighting parameter (α), this approach demonstrates both robustness and reliability for power quality disturbance detection.

These findings motivate further research into adaptive tuning strategies where α can be dynamically adjusted based on real-time noise estimation. In the future, this framework can be applied to real-time PQD features, using more advanced

Table 4. Adaptive Quantum-Classical Dual Kernel Performance on each Noise Levels

Noiseless					
Quantum		**Classical**		**Quantum-Classical Dual Kernel**	
K_q	Acc.(%)	K_c	Acc.(%)	K_{dual} with $\alpha^* = 0.4 - 1.0$	Accuracy
Linear	99.11	linear	97.01	Linear — poly	99.11%
Circular	98.82	poly	99.70		
Full	99.11	rbf	99.11		
50 dB SNR					
K_q	Acc.(%)	K_c	Acc.(%)	K_{dual} with $\alpha^* = 0.0 - 1.0$	Accuracy
Linear	100.0	linear	99.70	Linear — poly	100.0%
Circular	100.0	poly	100.0		
Full	99.70	rbf	100.0		
40 dB SNR					
K_q	Acc.(%)	K_c	Acc.(%)	K_{dual} with $\alpha^* = 0.0$	Accuracy
Linear	99.41	linear	99.70	Linear — linear	99.70%
Circular	99.41	poly	99.70		
Full	97.93	rbf	99.70		
30 dB SNR					
K_q	Acc.(%)	K_c	Acc.(%)	K_{dual} with $\alpha^* = 0.2$	Accuracy
Linear	98.82	linear	98.52	Linear — poly	100.0%
Circular	98.82	poly	99.41		
Full	97.63	rbf	98.22		
20 dB SNR					
K_q	Acc.(%)	K_c	Acc.(%)	K_{dual} with $\alpha^* = 0.45$	Accuracy
Linear	91.12	linear	92.31	Circular — poly	93.49%
Circular	92.90	poly	92.60		
Full	91.12	rbf	92.60		

techniques of detection. Additionally, extending the analysis to larger or more diverse datasets could help validate the scalability and generalizability of the dual kernel SVM approach. This work demonstrates the potential power of quantum computers in solving the challenges of renewable energy integration in future smart grids.

Disclosure of Interests. The authors have no competing interests to declare that are relevant to the content of this article.

References

1. Ahmed, S.D., Al-Ismail, F.S.M., Shafiullah, M., Al-Sulaiman, F.A., El-Amin, I.M.: Grid Integration Challenges of Wind Energy: A Review. *IEEE Access* **8**, 10857–10878 (2020). https://doi.org/10.1109/ACCESS.2020.2964896
2. Bendre, A., Divan, D., Kranz, W., Brumsickle, W.: Equipment Failures Caused by Power Quality Disturbances. In: *Conference Record of the 2004 IEEE Industry Applications Conference, 39th IAS Annual Meeting*, vol. 1, pp. 489. Seattle, WA, USA (2004). https://doi.org/10.1109/IAS.2004.1348450
3. Beniwal, R.K., Saini, M.K., Nayyar, A., Qureshi, B., Aggarwal, A.: A Critical Analysis of Methodologies for Detection and Classification of Power Quality Events in Smart Grid. *IEEE Access* **9**, 83507–83534 (2021). https://doi.org/10.1109/ACCESS.2021.3087016
4. Bhattacharyya, S., Myrzik, J.M.A., Kling, W.L.: Consequences of poor power quality – an overview. In: *2007 42nd International Universities Power Engineering Conference (UPEC)*, pp. 651–656. Brighton, UK (2007). https://doi.org/10.1109/UPEC.2007.4469025
5. Biamonte, J., Wittek, P., Pancotti, N., et al.: Quantum machine learning. *Nature* **549**, 195–202 (2017). https://doi.org/10.1038/nature23474
6. Borrás, M.D., Bravo, J.C., Montaño, J.C.: Disturbance Ratio for Optimal Multi-Event Classification in Power Distribution Networks. *IEEE Trans. Ind. Electron.* **63**(5), 3117–3124 (2016). https://doi.org/10.1109/TIE.2016.2521615
7. Caicedo, J.E., Agudelo-Martínez, D., Rivas-Trujillo, E., Meyer, J.: A Systematic Review of Real-Time Detection and Classification of Power Quality Disturbances. *Prot. Control Mod. Power Syst.* **8**(1), 1–37 (2023). https://doi.org/10.1186/s41601-023-00277-y
8. Cerqueira, A.S., Ferreira, D.D., Ribeiro, M.V., Duque, C.A.: Power quality events recognition using a SVM-based method. *Electr. Power Syst. Res.* **78**(9), 1546–1552 (2008). https://doi.org/10.1016/j.epsr.2008.01.016
9. Dulău, L.I., Abrudean, M., Bică, D.: Effects of Distributed Generation on Electric Power Systems. *Procedia Technology* **12**, 681–686 (2014). https://doi.org/10.1016/j.protcy.2013.12.549
10. Harker Steele, A.J., Burnett, J.W., Bergstrom, J.C.: The impact of variable renewable energy resources on power system reliability. *Energy Policy* **151**, 111947 (2021). https://doi.org/10.1016/j.enpol.2020.111947
11. Havlíček, V., Córcoles, A.D., Temme, K., et al.: Supervised learning with quantum-enhanced feature spaces. *Nature* **567**, 209–212 (2019). https://doi.org/10.1038/s41586-019-0980-2

12. IEEE: IEEE Recommended Practice for Monitoring Electric Power Quality. *IEEE Std 1159-2019 (Revision of IEEE Std 1159-2009)*, pp. 1–98 (2019). https://doi.org/10.1109/IEEESTD.2019.8796486
13. Igual, R., Miraftabzadeh, S., Foiadelli, F., Medrano, C.: Synthetic data of the paper: Quantification of feature importance in automatic classification of power quality distortions. *IEEE Dataport* (2019). https://doi.org/10.21227/bdqm-ds14
14. Igual, R., Miraftabzadeh, S.M., Foiadelli, F., Medrano, C.: Quantification of feature importance in automatic classification of power quality distortions. In: *2020 19th International Conference on Harmonics and Quality of Power (ICHQP)*, pp. 1–6 (2020). https://doi.org/10.1109/ICHQP46026.2020.9177897
15. Igual, R., Medrano, C., Arcega, F.J., Mantescu, G.: Integral mathematical model of power quality disturbances. In: *2018 18th International Conference on Harmonics and Quality of Power (ICHQP)*, pp. 1–6. Ljubljana, Slovenia (2018). https://doi.org/10.1109/ICHQP.2018.8378902
16. Javadi-Abhari, A., Treinish, M., Krsulich, K., Wood, C.J., Lishman, J., Gacon, J., Martiel, S., Nation, P.D., Bishop, L.S., Cross, A.W., Johnson, B.R., Gambetta, J.M.: Quantum computing with Qiskit. *arXiv preprint* arXiv:2405.08810 (2024). https://doi.org/10.48550/arXiv.2405.08810
17. Khan, T.M., Robles-Kelly, A.: Machine Learning: Quantum vs Classical. *IEEE Access* **8**, 219275–219294 (2020). https://doi.org/10.1109/ACCESS.2020.3041719
18. Lin, W.-m., Wu, C.-h., Lin, C.-h., Cheng, F.-s.: Classification of Multiple Power Quality Disturbances Using Support Vector Machine and One-versus-One Approach. In: *2006 International Conference on Power System Technology (ICPST)*, pp. 1–8. Chongqing, China (2006). https://doi.org/10.1109/ICPST.2006.321956
19. Mahela, O.P., Shaik, A.G., Gupta, N.: A critical review of detection and classification of power quality events. *Renew. Sustain. Energy Rev.* **41**, 495–505 (2015). https://doi.org/10.1016/j.rser.2014.08.070
20. Minh, H.Q., Niyogi, P., Yao, Y.: Mercer's Theorem, Feature Maps, and Smoothing. In: Lugosi, G., Simon, H.U. (eds) *Learning Theory. COLT 2006. Lecture Notes in Computer Science*, vol. 4005, Springer, Berlin, Heidelberg (2006). https://doi.org/10.1007/11776420_14
21. Pedregosa, F., Varoquaux, G., Gramfort, A., Michel, V., Thirion, B., Grisel, O., Blondel, M., Prettenhofer, P., Weiss, R., Dubourg, V., Vanderplas, J., Passos, A., Cournapeau, D., Brucher, M., Perrot, M., Duchesnay, É.: Scikit-learn: Machine Learning in Python. *J. Mach. Learn. Res.* **12**, 2825–2830 (2011). http://jmlr.org/papers/v12/pedregosa11a.html
22. Saini, M.K., Kapoor, R.: Classification of power quality events – A review. *Int. J. Electr. Power Energy Syst.* **43**(1), 11–19 (2012). https://doi.org/10.1016/j.ijepes.2012.04.045
23. Schuld, M.: Supervised quantum machine learning models are kernel methods. *arXiv preprint* arXiv:2101.11020 (2021). https://doi.org/10.48550/arXiv.2101.11020
24. Shin, Y., Parsons, A.C., Powers, E.J., Grady, W.M.: Time-frequency analysis of power system disturbance signals for power quality. In: *1999 IEEE Power Engineering Society Summer Meeting. Conference Proceedings*, vol. 1, pp. 402–407. Edmonton, AB, Canada (1999). https://doi.org/10.1109/PESS.1999.784382
25. Stockwell, R.G., Mansinha, L., Lowe, R.P.: Localization of the complex spectrum: the S transform. *IEEE Transactions on Signal Processing* **44**(4), 998–1001 (1996). https://doi.org/10.1109/78.492555

26. Tang, Q., Qiu, W., Zhou, Y.: Classification of Complex Power Quality Disturbances Using Optimized S-Transform and Kernel SVM. *IEEE Transactions on Industrial Electronics* **67**(11), 9715–9723 (2020). https://doi.org/10.1109/TIE.2019.2952823
27. Vita, V., Alimardan, T., Ekonomou, L.: The Impact of Distributed Generation in the Distribution Networks' Voltage Profile and Energy Losses. In: *2015 IEEE European Modelling Symposium (EMS)*, pp. 260–265. Madrid, Spain (2015). https://doi.org/10.1109/EMS.2015.46
28. Wang, Q.L., Jin, Y., Li, X.H., et al.: An advanced quantum support vector machine for power quality disturbance detection and identification. *EPJ Quantum Technol.* **11**, 70 (2024). https://doi.org/10.1140/epjqt/s40507-024-00283-5
29. Xu, T., Gao, W., Qian, F., Li, Y.: The implementation limitation of variable renewable energies and its impacts on the public power grid. *Energy* **239**(*Part A*), 121992 (2022). https://doi.org/10.1016/j.energy.2021.121992